Kramers problem in evolutionary strategies

J. Dunkel,* W. Ebeling, and L. Schimansky-Geier
Institut für Physik, Humboldt-Universität zu Berlin, Invalidenstrasse 110, D-10115 Berlin, Germany

P. Hänggi
Institut für Physik, Universität Augsburg, Institut für Physik, Theoretische Physik I, D-86135, Germany
(Received 10 December 2002; published 27 June 2003)

We calculate the escape rates of different dynamical processes for the case of a one-dimensional symmetric double-well potential. In particular, we compare the escape rates of a Smoluchowski process, i.e., a corresponding overdamped Brownian motion dynamics in a metastable potential landscape, with the escape rates obtained for a biologically motivated model known as the Fisher-Eigen process. The main difference between the two models is that the dynamics of the Smoluchowski process is determined by local quantities, whereas the Fisher-Eigen process is based on a global coupling (nonlocal interaction). If considered in the context of numerical optimization algorithms, both processes can be interpreted as archetypes of physically or biologically inspired evolutionary strategies. In this sense, the results discussed in this work are utile in order to evaluate the efficiency of such strategies with regard to the problem of surmounting various barriers. We find that a combination of both scenarios, starting with the Fisher-Eigen strategy, provides a most effective evolutionary strategy.

DOI: 10.1103/PhysRevE.67.061118 PACS number(s): 02.50.Ey, 82.20.Db, 02.60.Pn, 87.23.−n

I. INTRODUCTION

Since Kramers cornerstone paper on thermal activated barrier crossing [1] published in 1940, reaction rate theory has become an established discipline of nonlinear science, relevant in almost all scientific areas [2–5]. Alongside traditional problems from chemical reaction kinetics or electric transport theory, the problem of escape from metastable states has gained importance also in modern fields of science, such as evolutionary computation [6,7].

Generally, evolutionary numerical methods [8,9] were developed in order to solve complicated optimization problems, for instance, of the type

$$U(x) \overset{!}{=} \min \quad \text{or} \quad U(x) \overset{!}{=} \max, \tag{1}$$

where $U:\mathbb{R}^n \to \mathbb{R}$ and $n \gg 1$. A very recent application of evolutionary algorithms in the context of materials design was, for example, reported in Ref. [10]. With regard to nonphysical applications, function U can also be, e.g., a cost or fitness function. A physically motivated class of evolutionary algorithms, aiming at such problems, is constituted by the so-called thermodynamic strategies. These strategies are based on ensembles of overdamped Brownian particles and, thus, can be modeled by Smoluchowski equations [2,11,12]. Other, rather biologically oriented examples of evolutionary strategies include genetic algorithms [7] and also ensemble strategies with *global coupling* [13–17].

The essential connection between reaction rate theory and evolutionary optimization consists in the fact that in both cases the fundamental process is given by the transition between two neighboring wells or barriers, respectively. Thus, the methods developed in classical reaction theory (e.g., rate description, first passage time approach [2–4]) can also be successfully used in the characterization of evolutionary strategies.

In this paper we will conventionally confine ourselves to transitions between minima, since any maximum problem as given in Eq. (1) can be transformed into a minimum problem by simply exchanging the sign of U. Moreover, we shall adopt a physical point of view by considering function U as a ''physical potential.'' This is no restriction, because the generalization to nonphysical optimization problems is straightforward.

The primary objective of the present work is to compare a thermodynamic strategy featuring local coupling and a biological strategy based on global coupling with regard to transitions between metastable states. More precisely, we calculate the reaction rates of the biologically motivated Fisher-Eigen process for the symmetric Kramers potential, see Fig. 1, by use of the eigenvalue method, which is well-known from the classical escape rate theory [2]. As helpful guide in our calculations of the Fisher-Eigen escape rates, we shall

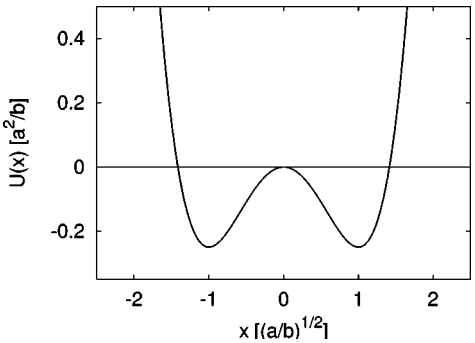

FIG. 1. Symmetric double-well potential $U(x) = -ax^2/2 + bx^4/4$ as used in the rate calculations performed below.

*Electronic address: dunkel@physik.hu-berlin.de

 ©2003 The American Physical Society

use the well-investigated Smoluchowski process. Since, as mentioned above, a Smoluchowski process can be interpreted as a thermodynamic evolutionary strategy [15–17], it will be interesting to compare the rates of the two processes from the point of view of evolutionary optimization. Put differently, we would like to inquire in what situations an algorithm with global coupling might be more efficient with regard to the problem of surmounting a barrier.

The two prototypes of evolutionary strategies that we plan to investigate are based on the idea that a statistical ensemble of pointlike objects or particles, respectively, move in the potential $U(x)$. In both cases the ensembles are described by a time-dependent, normalized probability density $p(x,t)$ possessing the common properties

$$p(x,t) \geqslant 0 \qquad \forall \;\; x \in \Omega, \;\; t \in T=[0,\infty), \tag{2a}$$

$$\int_{\Omega} dx p(x,t) = 1 \qquad \forall \;\; t \in T. \tag{2b}$$

Thus, for both strategies the total number of ensemble members is conserved; and $p(x,t)dx$ characterizes the fraction of the ensemble in the interval $[x,x+dx]$ of the search space $\Omega \subseteq \mathbb{R}^n$ at time t. The main difference between the two models is given by the underlying principles (or selection schemes), according to which the ensembles evolve on the potential landscape $U(x)$.

We start with the Smoluchowski dynamics that corresponds to overdamped Brownian motion. Without loss of generality, it is sufficient for the subsequent discussion when we consider the one-dimensional case.

The dynamics of overdamped Brownian particles can be described by the overdamped Langevin equation [2,12]

$$m\gamma \frac{dx}{dt} = -\nabla U(x) + \xi(t), \tag{3}$$

where m denotes the mass of the Brownian particles, γ is the viscous friction coefficient, and $\xi(t)$ is a δ-correlated Gaussian random force (white noise) characterized by

$$\langle \xi(t) \rangle = 0, \qquad \langle \xi(t)\xi(s) \rangle = 2\, m\gamma\, k_B T \delta(t-s). \tag{4}$$

As usual, we have denoted Boltzmann's constant by k_B, and T is the temperature of the heat bath modeled by $\xi(t)$. An equivalent description of the Langevin dynamics (3) is given by Smoluchowski's equation [2,11,12]

$$\frac{\partial p}{\partial t} = \frac{1}{m\gamma} \nabla [(\nabla U) p] + \frac{k_B T}{m\gamma} \nabla^2 p. \tag{5}$$

The parameter

$$D \equiv \frac{k_B T}{m\gamma} \tag{6}$$

in Eq. (5) is the diffusion constant, or noise strength, respectively. Note that Smoluchowski's equation is a local equation in the sense that only local properties of $U(x)$ and $p(x,t)$ influence the dynamics of the ensemble.

In contrast to the Smoluchowski process, the biologically motivated Fisher-Eigen process [13,14,18] is based on global selection, i.e., members of the ensemble are reproduced or destroyed according to their status in the overall ensemble. The evolutionary equation of this model is the generalized Fisher-Eigen equation, reading

$$\frac{\partial p}{\partial t} = q[\overline{U}(t) - U] p + D \nabla^2 p, \tag{7}$$

where

$$\overline{U}(t) = \int_{\Omega} dx U(x) p(x,t) \tag{8}$$

is the time-dependent ensemble average of U and $q>0$ a coupling parameter. Note that the Fisher-Eigen equation (7) constitutes a nonlinear partial differential equation (PDE), whereas the Smoluchowski equation (5) is linear. The effect of the selective first term on the right-hand side (rhs) of Eq. (7) is obvious. It leads to an increase of the local population, if value $U(x)$ is lower than the ensemble average $\overline{U}(t)$ and to a decrease, otherwise. In clear contrast to the local Smoluchowski equation (5), we have a nonlocal selection criterion in the case of Eq. (7); i.e., the change of the local population in $[x,x+dx]$ between t and $t+dt$ can also be strongly influenced by those parts of the overall population which are located at far distances from x. In this sense, the models with a nonlocal selection scheme are always based on the assumption that the corresponding system includes long-ranging information transfer mechanisms as a fundamental feature. It comes at no surprise that typical examples exhibiting such global coupling mechanisms are biological systems.

We note that in previous papers [15–17] dealing with these two evolutionary models, the Smoluchowski process was also referred to as a thermodynamic ''Boltzmann strategy'' and the Fisher-Eigen process as ''Darwin strategy.'' Furthermore, we would like to mention that numerical methods realizing Eq. (5) are, for example, based on a discretized version of the Langevin equation (3); whereas the selection scheme of the Fisher-Eigen process can be realized via reaction mechanisms as known from the description of chemical reactions. For a detailed discussion of this issue, including applications to optimization problems (e.g., optimization of road networks), we refer the reader to Refs. [16,19–21].

We next present a brief overview of the structure of this paper. In the explicit rate calculations performed below, we exclusively concentrate on one-dimensional problems; more exactly, we are interested in transitions between the wells of the symmetric Kramers potential

$$U(x) = -\frac{a}{2}x^2 + \frac{b}{4}x^4, \qquad a,b>0, \tag{9}$$

which is shown in Fig. 1.

Because, for the Smoluchowski equation, the rate problem for the Kramers potential (9) has been extensively studied in the past [1–4,12], our primary aim is to derive corresponding analytic expressions for the reaction rate of the

Fisher-Eigen problem by following a similar sequence of steps. In order to clarify the analogies in the derivation, we first outline the well-known calculation of the reaction rate for the Smoluchowski equation.

The paper is organized as follows. In Sec. II, general solution techniques are briefly reviewed, which are put to use later on in Sec. III wherein we evaluate the escape rates. Section IV comprises a summary of the main results and conclusions. In Appendix C the details on numerical methods applied to the corresponding PDE are given.

II. GENERAL SOLUTION TECHNIQUES

The Smoluchowski equation (5) was derived in 1915 by von Smoluchowski [11] in order to describe the motion of overdamped Brownian particles in an external potential $U(x)$. Since, this equation has been studied in detail for different types of potential functions $U(x)$, and we shall make use of results presented in Refs. [2,12,22] during our subsequent discussion. Furthermore, for the Fisher-Eigen process, some results can be found in Ref. [18].

The essence of this section can be summarized as follows: Both, the Smoluchowski equation as well as the Fisher-Eigen equation can be transformed into a Schrödinger equation.

A. Smoluchowski equation

To start, it is useful to introduce dimensionless quantities

$$\tilde{x}\equiv\frac{x}{x_m},\quad \tilde{t}\equiv\frac{t\,a}{m\gamma},\quad \tilde{D}\equiv\frac{k_BT}{a\,x_m^2},\quad \tilde{p}(\tilde{x},\tilde{t})\equiv p(x,t)x_m, \tag{10}$$

where $x_m=+\sqrt{a/b}$ is the distance between the maximum and minimum of the Kramers potential (9). Dropping, for the sake of convenience, all tildes we can rewrite the Smoluchowski equation (5) in dimensionless form

$$\frac{\partial p}{\partial t}=\boldsymbol{\nabla}[(x^3-x)p]+D\nabla^2 p, \tag{11}$$

corresponding to the motion in the rescaled (dimensionless) Kramers potential

$$U(x)=\tfrac{1}{4}x^4-\tfrac{1}{2}x^2. \tag{12}$$

As one can readily check upon an insertion, the stationary solution of Eq. (11) is given by the Boltzmann distribution

$$p^{st}(x)=\frac{e^{-U(x)/D}}{\mathcal{Z}^{st}}, \tag{13}$$

where

$$\mathcal{Z}^{st}=\int_\Omega dx e^{-U(x)/D} \tag{14}$$

is the stationary normalization constant. Equation (13) is the reason why the process described by Eq. (11) is sometimes also termed the thermodynamical Boltzmann strategy. Since $p^{st}(x)$ possesses maxima at the minima of $U(x)$, the Smoluchowski process can be considered as an optimization strategy. In order to construct time-dependent solutions of Eq. (11), it is convenient to use the ansatz [18]

$$p(x,t)=\varrho(x,t)\exp\left[-\frac{U(x)}{2D}\right]. \tag{15}$$

Inserting this very ansatz into Eq. (11) leads to

$$\frac{\partial\varrho}{\partial t}=D\nabla^2\varrho-\left[\frac{1}{4D}(\boldsymbol{\nabla}U)^2-\frac{1}{2}\nabla^2U\right]\varrho. \tag{16}$$

Mathematically, Eq. (16) can be treated as a Schrödinger equation [23–25]. Thus, assuming a discrete spectrum of eigenvalues, the complete solution of Eq. (11) can be expressed in terms of the series expansion

$$p(x,t)=\exp\left[-\frac{U(x)}{2D}\right]\sum_{n=0}^{\infty}c_n\phi_n(x)e^{-\lambda_n t}, \tag{17}$$

where λ_n are the eigenvalues of the Hamilton operator

$$\hat{H}_S=-D\nabla^2+v(x),\qquad v(x)=\frac{1}{4D}(\boldsymbol{\nabla}U)^2-\frac{1}{2}\nabla^2U \tag{18}$$

with corresponding time-independent eigenfunctions $\phi_n(x)$. Assuming $L^2(\Omega)$-normalized eigenfunctions $\phi_n(x)$, i.e.,

$$(\phi_n,\phi_m)\equiv\int_\Omega dx\,\phi_n^*(x)\phi_m(x)=\delta_{nm}, \tag{19}$$

the coefficients c_n in Eq. (17) are determined by the initial condition

$$c_n=(\phi_n,\varrho_0)=\int_\Omega dx\,\phi_n^*(x)\exp\left[\frac{U(x)}{2D}\right]p(x,0), \tag{20}$$

where $\varrho_0(x)=\varrho(x,0)$. Furthermore, for $t\to\infty$, the series expansion (17) must converge to the stationary solution (13). Thus one finds that $\lambda_0=0$, $c_0=1/\sqrt{\mathcal{Z}^{st}}$, and

$$\phi_0(x)=\frac{e^{-U(x)/2D}}{\left[\int_\Omega dz\,e^{-U(z)}\right]^{1/2}}=\frac{e^{-U(x)/2D}}{\sqrt{\mathcal{Z}^{st}}}. \tag{21}$$

Hence, as we can immediately see from Eq. (17), for $t\gg0$ the eigenvalue λ_1 dominates the dynamics of density $p(x,t)$.

We note that although the solution of the Smoluchowski equation is formally known by Eq. (17), it is of use, only in parts, in more complicated applications. This is due to the fact that apart from some very simple potentials U, the eigenvalues and eigenfunctions of the Hamilton operator (18) with the effective potential v are unknown.

For the rescaled potential (12) the effective potential $v(x)$ is given by

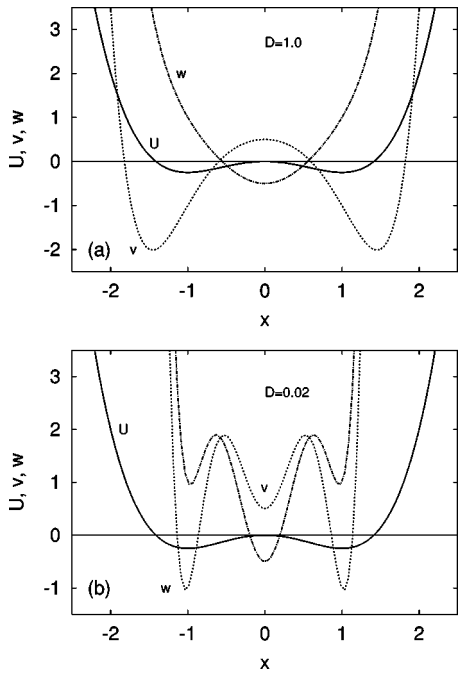

FIG. 2. Double-well potential $U(x)=x^4/4-x^2/2$, and the corresponding effective potential $v(x)$ and supersymmetric partner potential $w(x)$ of $v(x)$ as used in the calculation of the eigenvalue λ_1. (a) For strong noise strength $D\geqslant 1/6$, the effective potential $v(x)$ exhibits also a double-well potential structure and for $D\geqslant 1/18$ the fermionic partner potential $w(x)$ becomes monostable. (b) In the case of $D<1/6$, the shape of the effective potential $v(x)$ is essentially different from the shape of $U(x)$.

$$v(x)=\frac{1}{4D}(x^3-x)^2-\frac{1}{2}(3x^2-1). \tag{22}$$

We shall need it later, since, as briefly reviewed in Sec. III, the escape rate is closely related to the first nonvanishing eigenvalue λ_1. In Fig. 2 we have depicted both $u(x)$ and $v(x)$ for different noise strengths D. Given the Taylor expansion

$$v(x)=\frac{1}{2}+\frac{1}{4D}(1-6\,D)x^2+O(x^4) \tag{23}$$

at $x=0$, we deduce that $v(x)$, as given in Eq. (22), is a double-well potential only as long as

$$D\geqslant\tfrac{1}{6}. \tag{24}$$

Otherwise, $v(x)$ possesses three minima, see Fig. 2(b). Moreover, the supersymmetric (fermionic) partner potential [22,26,27]

$$w(x)\equiv\frac{1}{4D}(\boldsymbol{\nabla}U)^2+\frac{1}{2}\nabla^2U=\frac{1}{4D}(x^3-x)^2+\frac{1}{2}(3x^2-1) \tag{25}$$

is monostable as long as $D\geqslant 1/18$. In order to obtain a simple estimate of the eigenvalue λ_1 in the strong noise limit $D\gg 0$, we also need the frequency

$$\nu=\sqrt{3+\frac{1}{2D}} \tag{26}$$

of w at the bottom of the well at $x=0$.

B. Fisher-Eigen process

Before we discuss solutions of the Fisher-Eigen equation (7)

$$\frac{\partial p}{\partial t}=q[\overline{U}(t)-U]p+D\nabla^2p,$$

it is advantageous to introduce dimensionless quantities

$$\tilde{x}\equiv\frac{x}{x_m},\qquad \tilde{t}\equiv t\,q\,a\,x_m^2,\qquad \tilde{D}\equiv\frac{D}{q\,a\,x_m^4},$$

$$\tilde{p}(\tilde{x},\tilde{t})\equiv p(x,t)x_m. \tag{27}$$

By virtue of these transformations the form of the rescaled (dimensionless) Kramers potential is given by Eq. (12), i.e., $\tilde{U}(\tilde{x})=\tilde{x}^4/4-\tilde{x}^2/2$. For the sake of convenience, we drop again all tildes from now on and obtain the following dimensionless version of the Fisher-Eigen equation (7):

$$\frac{\partial p}{\partial t}=[\overline{U}(t)-U]p+D\nabla^2p. \tag{28}$$

We have already mentioned that in contrast to the Smoluchowski equation (11), the generalized Fisher-Eigen equation (28) is a nonlinear PDE. Nevertheless, it can also be transformed into a PDE of Schrödinger type (16) by using the ansatz [18]

$$p(x,t)=\varrho(x,t)\exp\left[\int_0^t\overline{U}(s)ds\right], \tag{29}$$

where in contrast to the probability density $p(x,t)$ the auxiliary function $\varrho(x,t)$ stays not normalized. Inserting ansatz (29) into Eq. (28), one finds the result

$$\frac{\partial\varrho}{\partial t}=D\nabla^2\varrho-U\varrho. \tag{30}$$

Compared with Eq. (16) the essential difference consists in the fact that instead of the effective potential $v(x)$ in Eq. (16), the original potential $U(x)$ appears in Eq. (30). Thus, assuming a discrete spectrum of eigenvalues again, the formal solution of Eq. (28) reads

$$p(x,t)=\exp\left[\int_0^t\overline{U}(s)ds\right]\sum_{n=0}^{\infty}c_n\phi_n(x)e^{-\lambda_n t}, \tag{31}$$

where ϕ_n is a $L^2(\Omega)$-normalized eigenfunction of the Hamilton operator

$$\hat{H}_{\mathrm{FE}}=-D\nabla^2+U(x) \tag{32}$$

and λ_n is the corresponding eigenvalue. The coefficients

$$c_n = \int_\Omega dx\, \phi_n^*(x) p(x,0) \tag{33}$$

are again determined by the initial condition. In order to identify the prefactor in Eq. (31), we can use the fact that $p(x,t)$ stays normalized at all times t. More precisely, we can integrate Eq. (31) over x, yielding

$$1 = \exp\left[\int_0^t \overline{U}(s)ds\right] \sum_{n=0}^{\infty} c_n l_n e^{-\lambda_n t}, \tag{34}$$

wherein we defined the coefficients

$$l_m = \int_\Omega dx\, \phi_m(x). \tag{35}$$

Therefore, the final result for the probability density (31) can be written as

$$p(x,t) = \frac{\sum_{n=0}^{\infty} c_n \phi_n(x) e^{-\lambda_n t}}{\sum_{m=0}^{\infty} c_m l_m e^{-\lambda_m t}}. \tag{36}$$

Put differently, the solution of the generalized Fisher-Eigen problem (28) can be expressed in terms of characteristic quantities of the eigenvalue problem (30). Moreover, by virtue of (34) we also immediately obtain

$$\overline{U}(t) = -\frac{d}{dt}\ln \sum_{n=0}^{\infty} c_n l_n e^{-\lambda_n t} = \frac{\sum_{n=0}^{\infty} c_n l_n \lambda_n e^{-\lambda_n t}}{\sum_{m=0}^{\infty} c_m l_m e^{-\lambda_m t}}, \tag{37}$$

and the additional condition

$$\sum_{n=0}^{\infty} c_n l_n = 1. \tag{38}$$

The latter result follows from Eq. (34) by setting $t=0$. Also note that in the case of the symmetric double-well potential considered below, $l_n = 0$ holds if $n = odd$. This is due to the symmetry properties of the eigenfunctions ϕ_n of $\hat{H}_{\mathrm{FE}}$.

Let us now still have a closer look at the stationary situation. Assuming a time-independent solution $p^{st}(x)$ of Eq. (28) for $t \to \infty$, we find from the rhs of Eq. (37) that the stationary value $\overline{U}^{st}$ of $\overline{U}(t)$ is given by the lowest eigenvalue

$$\overline{U}^{st} = \lambda_0, \tag{39}$$

and, furthermore, from Eq. (36) that the stationary solution $p^{st}(x)$ is proportional to $\phi_0(x)$, i.e.,

$$p^{st}(x) = \frac{\phi_0(x)}{\mathcal{Z}^{st}}, \tag{40}$$

where $\mathcal{Z}^{st} = l_0$.

On the basis of the exact solutions (17) and (36), we are now able to calculate approximate analytic expressions for the escape rates of both processes, which will be the subject of the following section.

III. CROSSING OVER A BARRIER

In this section we study the following problem. We consider Kramers symmetric double-well potential (9), and all members of the ensemble initially situated at the bottom of the left well, i.e., at $x=-1$. Using, as in the previous sections, dimensionless quantities, this special initial condition corresponds to

$$p(x,0) = \delta(x+1). \tag{41}$$

The quantity we intend to estimate analytically is the escape rate k characterizing the decline of the population in the left well or the increase of the population in the right well. The population in the left well, denoted by p_-, and that in the right well, denoted by p_+, are given by

$$p_-(t) \equiv \int_{-\infty}^{0} dx p(x,t), \qquad p_+(t) \equiv \int_0^{+\infty} dx p(x,t), \tag{42}$$

and from Eq. (41) follow the initial conditions $p_-(0)=1$ and $p_+(0)=0$. Of course, for Smoluchowski and Fisher-Eigen processes, the dynamics of $p_\pm(t)$ is governed by the respective evolutionary equation for $p(x,t)$ and can be evaluated numerically. However, in order to derive also analytical estimates, it is appropriate to approximate the actual process by the following set of (two-state) master equations:

$$\dot{p}_- = -k\, p_- + k\, p_+ \tag{43a}$$

$$\dot{p}_+ = k\, p_- - k\, p_+, \tag{43b}$$

where $\dot{p}_\pm = dp_\pm/dt$. The quantity k, appearing on the rhs of Eqs. (43) is the escape rate, respectively. Note, that only because of the symmetric test potential chosen here, the rates for the left and right wells are identical. As one can easily check, the solution of Eq. (43) reads

$$p_\pm(t) = p_\pm^\infty + [p_\pm(0) - p_\pm^\infty]\exp(-2k\,t), \tag{44}$$

where $p_\pm^\infty$ represents the respective stationary value. For our symmetric double-well potential $p_\pm^\infty = 1/2$, and we can rewrite Eq. (44) in the simplified form

$$p_\pm(t) = \tfrac{1}{2} \mp \tfrac{1}{2}\exp(-2k\,t). \tag{45}$$

Apparently, the escape rate k can be considered as a measure for the ability of a certain strategy to surmount a barrier, i.e., we assess that strategy X is *"more mobile"* than strategy Y, if

$$k^X > k^Y \tag{46}$$

is true.

A. Rates for the Smoluchowski process

In principle, for the Smoluchowski process, several excellent analytical estimates for the escape rate k^{S} are known, which are based on different approximation techniques (e.g., eigenvalue method, flux over population method) [2]. Since the eigenvalue method turns out to be successfully applicable to the Smoluchowski as well as to the Fisher-Eigen strategy, we shall briefly outline this method by means of the Smoluchowski process in the following, where the case of strong noise is discussed. Later on, in Sec. III B, we also give a well-known rate result for the opposite case of weak noise, which is based on the stationary flux method [2].

(a) Strong noise (eigenvalue method). Using the solution (17) of the Smoluchowski equation (11) we can write

$$p_-(t) = \frac{1}{2} + \int_{-\infty}^{0} dx e^{-U(x)/2D} \sum_{n=1}^{\infty} c_n \phi_n(x)\, e^{-\lambda_n t}. \tag{47}$$

Thus, for $t \gg 0$ we find asymptotically

$$p_-(t) \cong \frac{1}{2} + \exp(-\lambda_1 t) \int_{-\infty}^{0} dx e^{-U(x)/2D} c_1 \phi_1(x), \tag{48}$$

where according to Eqs. (20) and (41)

$$c_1 = \int_{-\infty}^{\infty} dx \phi_1^*(x) e^{U(x)/2D} p(x,0) = \phi_1^*(-1) e^{U(-1)/2D}. \tag{49}$$

For the special initial condition (41), we can estimate

$$\int_{-\infty}^{0} dx c_1 \phi_1(x) e^{-U(x)/2D} \approx \int_{-\infty}^{0} dx c_0 \phi_0(x) e^{-U(x)/2D} = \frac{1}{2}, \tag{50}$$

because $\phi_0(x) \approx \phi_1(x)$ holds in the vicinity of $x=-1$ [we assumed additionally a normalization such that $\phi_1(x) > 0$ for $x < 0$]. Upon inserting this estimate into Eq. (48) and comparing the result with Eq. (45), we can expect that for the Smoluchowski process the rate is approximately given by

$$k^S = \frac{\lambda_1}{2}, \tag{51}$$

where λ_1 is the lowest nonvanishing eigenvalue of the Hamilton operator (18). Since, as mentioned earlier, $\lambda_0 = 0$ holds, we could also write $k^S = \Delta\lambda/2$, where $\Delta\lambda \equiv \lambda_1 - \lambda_0$ is the difference between the lowest two eigenvalues.

Unfortunately, it is generally impossible to determine λ_1 exactly for the effective potential $v(x)$ from Eq. (22), and one has to employ approximation techniques, e.g., WKB or supersymmetric (SUSY) methods as known from quantum mechanics and widely applied in statistical physics [2,22,26–30]. Using SUSY methods, one finds by quadratic approximation for relatively strong noise

$$D \gg 1/18, \tag{52}$$

the rate

$$k^S_{\mathrm{susy}} = -\frac{1}{4} + \frac{\sqrt{2D}}{4}\nu = -\frac{1}{4} + \frac{1}{4}\sqrt{6D+1}, \tag{53}$$

where ν was defined in Eq. (26) as the frequency of the fermionic partner potential $w(x)$ at $x=0$. In Fig. 3(a) one can contemplate that for strong noise $D \geqslant 1$ the analytical approximation, given by k^S_{susy} inserted into Eq. (45), yields good agreement with numerical results based on simulations of the PDE (11). Details regarding the numerical simulation of the PDE are presented in Appendix C.

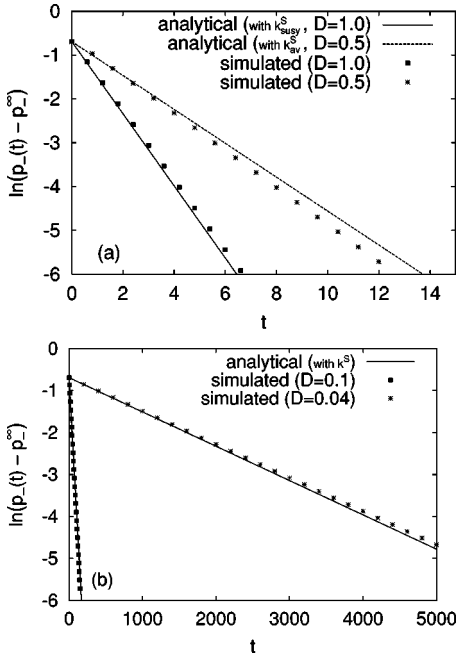

FIG. 3. Semilogarithmic plots of the decrease of the population $p_-(t)$ in the left well (reduced by its stationary value $p_-^\infty = 0.5$) for the Smoluchowski process. (a) Strong and moderate noise: For the analytical curves we used the rate expression k^S_{susy} from Eq. (53), and the rate k^S_{av} from Eq. (57), respectively. (b) Weak noise: Both analytical graphs are based on the rate k^{S} as given in Eq. (56).

(b) Moderate to weak noise strength. As already mentioned, there exist many results obtained by working directly with the Smoluchowski equation [2]. Here we shall apply some of them to our rescaled dimensionless stochastic dynamics. A general result based on the stationary flux method is given by the following integral formula for the inverse rate [2]:

$$(k^S)^{-1} = \frac{1}{D} \int_{-\infty}^{0} dy \exp\left[-\frac{U(y)}{D}\right] \int_{y}^{\infty} dz \exp\left[\frac{U(z)}{D}\right]. \tag{54}$$

We remark that this result may as well be derived by a mean first time passage time approach [2]. In the case of weak noise

$$\frac{\Delta U}{D}=\frac{1}{4D}\gg 1, \tag{55}$$

one can evaluate Eq. (54) by a Gaussian steepest-descent approximation, yielding the dimensionless estimate [2]

$$k^S=\frac{\omega_0\omega_b}{2\pi}\exp\left(-\frac{\Delta U}{D}\right)\left[1-\frac{3}{2}D+O(D^2)\right], \tag{56}$$

where $\Delta U=1/4$ is the depth of the rescaled double-well potential, $\omega_0=\sqrt{2}$ is the dimensionless angular frequency at the bottom of the minimum at $x=-1$, and $\omega_b=1$ is the dimensionless angular frequency at the top of the barrier at $x=0$. The prefactor before the brackets corresponds to the well-known Kramers result [1,2] valid for strong damping (that is, very weak noise $D\to 0$). In Fig. 3(b) one can see that the corresponding analytical approximation, given by k^{S} inserted into Eq. (45), is in good agreement with the numerically calculated relaxation dynamics as long as $D\leqslant 0.1$ holds, which is in accordance with weak noise.

In the intermediate region of moderate noise strength, $0.1\leqslant D\leqslant 1.0$, the average escape rate

$$k^S_{\mathrm{av}}\equiv\frac{1}{2}\left[k^S_{\mathrm{susy}}+\frac{1}{\sqrt{2}\,\pi}\exp\left(-\frac{\Delta U}{D}\right)\right] \tag{57}$$

yields satisfactory analytical estimates for the simulated decay curves, see Fig. 3(a).

B. Rates for the Fisher-Eigen process

Having discussed the rate problem for the Smoluchowski process, we next address the Fisher-Eigen process. Before we can actually calculate a rate k^{FE} for the Fisher-Eigen model, it is again necessary to take a closer look at the asymptotic behavior of this strategy. For $t\gg 0$, the lowest lying eigenvalues dominate the numerator and the denominator of the time-dependent solution (36). If we neglect terms $n,m\geqslant 2$ in Eq. (36) and also consider the well-known fact that for symmetric potentials the first eigenfunction is asymmetric, $\phi_1(x)=-\phi_1(-x)$, which again leads to $l_1=0$, we attain the asymptotic solution

$$p(x,t)\cong\frac{\phi_0(x)}{l_0}+\frac{c_1\,\phi_1(x)}{c_0\,l_0}e^{-(\lambda_1-\lambda_0)t}. \tag{58}$$

For the special initial condition (41) and sufficiently weak noise, we can approximate $c_1\approx c_0=\phi_0(-1)$ and

$$\int_{-\infty}^{0}dx\,\phi_0(x)\approx\int_{-\infty}^{0}dx\,\phi_1(x)=\frac{l_0}{2}. \tag{59}$$

Thus, we find

$$k^{\mathrm{FE}}=\tfrac{1}{2}(\lambda_1-\lambda_0)=\tfrac{1}{2}\Delta\lambda \tag{60}$$

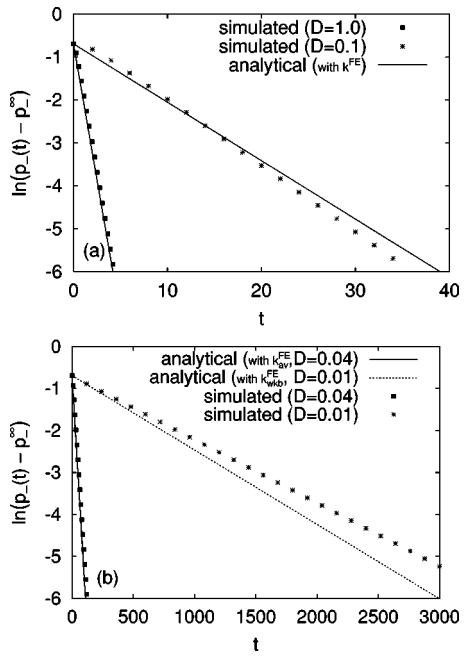

FIG. 4. Semilogarithmic plots of the decay curves of the population $p_-(t)$ in the left well (reduced by the stationary value $p_-^{\infty}=0.5$) for the Fisher-Eigen process. (a) Strong noise: For the analytical curves the rate k^{FE} from Eq. (65) was used. (b) Moderate and weak noise: Here the analytical graphs are based on $k^{\mathrm{FE}}_{\mathrm{av}}$ as given in Eq. (66), and $k^{\mathrm{FE}}_{\mathrm{wkb}}$ as given in Eq. (62). Note that compared with the Smoluchowski process, see Fig. 3(b), the Fisher-Eigen process is ''more mobile'' at moderate to weak noise corresponding to parameter values $D\leqslant 1.0$.

for the escape rate for the Fisher-Eigen process. Before we proceed, we would like to emphasize again that, in contrast to the Smoluchowski rate k^{S}, the eigenvalues appearing in Eq. (60) are those of the Hamilton operator $\hat{H}_{\mathrm{FE}}$ containing the original potential $U(x)$.

Of course, the problem of calculating the eigenvalue difference $\Delta\lambda$ for the double-well potential U is a key problem in quantum mechanics, see Refs. [26,29–31], and also references therein. For small dimensionless noise parameters

$$D\leqslant 1/16, \tag{61}$$

a WKB approximation (see Appendix A for details) yields the rate

$$k^{\mathrm{FE}}_{\mathrm{wkb}}=\frac{D^{1/2}}{\pi}\exp\left(-\frac{2\,\Phi}{D^{1/2}}\right), \tag{62}$$

where

$$\Phi=\frac{1}{3}z_2\left[\mathcal{E}\left(\frac{z_1^2}{z_2^2}\right)-2D^{1/4}\mathcal{K}\left(\frac{z_1^2}{z_2^2}\right)\right] \tag{63}$$

and

$$z_1=\sqrt{1-2D^{1/4}},\qquad z_2=\sqrt{1+2D^{1/4}}. \tag{64}$$

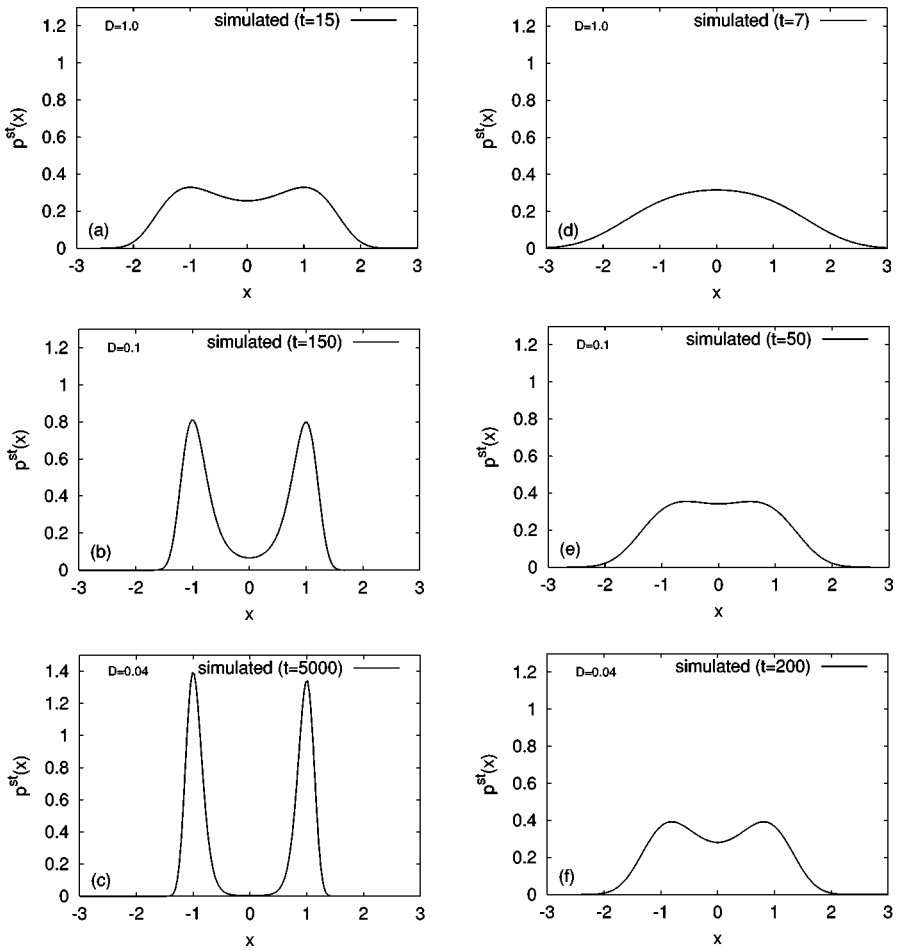

FIG. 5. Comparison of the numerically calculated ''stationary'' solutions (taken at time t as given in the diagrams) for the particle density. It becomes obvious that the stationary solutions of the Smoluchowski process, represented in diagrams (a)–(c), possess much better properties with regard to ensemble minima search than those of the Fisher-Eigen process given in (d)–(f).

Furthermore, $\mathcal{K}$ and $\mathcal{E}$ denote the complete elliptic integrals of the first and the second kind, respectively, as defined in Eqs. (A9) and (A10). In the limit of very weak noise $D \to 0$, one finds $\Phi \to 1/3$. Compared with the Smoluchowski process the essential observation is that at small noise parameters $D \ll 1$ the Fisher-Eigen process is more mobile than the Smoluchowski process. Put differently, in the weak noise regime the global selection criterion turns out to be much more efficient for the process of overcoming a barrier.

In the opposite case of strong noise strength, we obtain from the standard time-independent perturbation theory (see Appendix B)

$$k^{\mathrm{FE}} = \left(\frac{3D^2}{4}\right)^{1/3} - \left(\frac{D}{48}\right)^{1/3}. \tag{65}$$

This approximation can principally be valid only as long as $D > 1/36$, because otherwise the rate would assume negative values. As shown in Fig. 4(a) this estimate for rate (65) can successfully be applied to describe the relaxation dynamics of the population $p_-(t)$ if $D \geqslant 0.1$.

As before, in the case of the Smoluchowski process, there exists an intermediate region, now corresponding to $1/36 \leqslant D \leqslant 0.1$, where the average rate

$$k_{\mathrm{av}}^{\mathrm{FE}} \equiv \tfrac{1}{2}(k^{\mathrm{FE}} + k_{\mathrm{wkb}}^{\mathrm{FE}}) \tag{66}$$

yields a satisfactory analytical estimate of the numerical results, see Fig. 4(b).

C. Comparison of the stationary solutions

With regard to evolutionary optimization, it is not only important which of the two strategies approaches its stationary distribution most rapidly. One certainly also needs to know about the quality of the stationary distributions. In the context of a computational optima search those strategies are to be favored where, in the stationary state, the majority of the members of the search ensemble is located near the optimum.

In Fig. 5 we have depicted the stationary probability densities for the Smoluchowski and the Fisher-Eigen processes, based on simulations with identical parameters. As one can clearly deduce from the results, the stationary distribution of the Smoluchowski process possesses advantageous properties as compared to the corresponding Fisher-Eigen process. In particular, the stationary distribution of the latter process possesses only a single maximum at the barrier $x = 0$, if the dimensionless noise strength becomes sufficiently large.

This observation means that we face a situation typically referred to as ''frustrated problem.'' On the one hand, the Fisher-Eigen process is more mobile than the Smoluchowski

scenario, i.e., it is more efficient if a barrier of the landscape must be crossed. In contrast, the stationary probability density is lesser peaked at the minima of the potential. A quantitative explanation for this effect based on the special case with harmonic potentials can be found in Ref. [32]. There it was shown that the two processes exhibit different functional dependencies between the angular frequency at the minimum and the variance of the stationary distribution.

IV. CONCLUSIONS

In this work we have calculated and compared escape rates of the Smoluchowski and Fisher-Eigen processes by applying the eigenvalue method. While the escape problem is well investigated in the Smoluchowski case, the results obtained for the Fisher-Eigen strategy are not so.

Even though we confined our quantitative discussion to the one-dimensional symmetric Kramers potential, the results seemingly indicate some rather general and robust properties of the two strategies. As we have discovered from our rate calculations in Sec. III, for weak (dimensionless) noise strength D, the Fisher-Eigen process with global selection is much more efficient if a barrier has to be overcome. We are confident that this property remains true also for high-dimensional problems. The main reason for this conjecture is that with regard to high-dimensional search spaces, the one-dimensional model represents a good approximation for the ensemble dynamics in the vicinity of the shortest link between two neighboring optima.

Moreover, in a different investigation of the two models for a simple harmonic potential, we could establish [32] that for sufficiently low noise parameters the stationary solution of the Smoluchowski process possesses better properties regarding the local concentration of the stationary distribution around a minimum. Thus, from the evolutionary optimization point of view we herewith do recommend the following combination of the two strategies: (1) To start with, use the Fisher-Eigen process in the beginning of the search process; (2) then switch to a local Smoluchowski process (with very small D) at the final stages.

Finally, we would like to comment on the approach chosen in this paper. Obviously, in the general case it *is not possible* to transform the Schrödinger equation into a Smoluchowski equation, albeit one can always transform a Smoluchowski equation into an equation of Schrödinger type (the latter result was first discovered by Favella [24]). This nonequivalence of the Smoluchowski and Schrödinger equations is also evident in the case of the Fisher-Eigen process where the eigenvalue method is thus far the only technique allowing for an estimate of the crossing dynamics. From this point of view, the Smoluchowski process is technically simpler and we actually can choose from several different techniques [2]. In particular, there also exists a great variety of suitable methods such as the MFPT-approach, the stationary flux method, etc., to name but a few, which generally yield superior results over the WKB approximation that is rooted in quantum mechanics. However, when we are interested in evolutionary strategies of the Fisher-Eigen type, we exclusively depend on such an eigenvalue analysis.

ACKNOWLEDGMENTS

This work was supported by the DFG via Grant Nos. Sfb-555 (L.S.-G. and J.D.), Sfb-486 (P.H.), and by the Studienstiftung des deutschen Volkes (J.D.).

APPENDIX A: WKB APPROXIMATION FOR THE FISHER-EIGEN PROCESS

The eigenvalue problem corresponding to Eq. (30) reads

$$\lambda\phi = -D\phi_{xx} + U\phi, \qquad U = -\tfrac{1}{2}x^2 + \tfrac{1}{4}x^4. \tag{A1}$$

In the WKB approximation the eigenvalue difference $\Delta\lambda = \lambda_1 - \lambda_0$ is given by

$$\Delta\lambda = \frac{\sqrt{2}D^{1/2}\omega_0}{\pi}\exp\left[-\frac{2}{D^{1/2}}\int_0^{z_1} dx\sqrt{U(x)-\varepsilon_0}\right], \tag{A2}$$

where

$$\varepsilon_0 = -\tfrac{1}{4} + D^{1/2} \tag{A3}$$

is the ground-state eigenvalue obtained for the parabolic approximation of $U(x)$ at the minimum at $x=1$, and $\omega_0=\sqrt{2}$ is the corresponding dimensionless angular frequency. Further, the upper boundary z_1 of the integral corresponds to the smallest, positive solution of the problem

$$G(z) \equiv \sqrt{U(z)-\varepsilon_0} = 0. \tag{A4}$$

The positive solutions of Eq. (A4) are

$$z_1 = \sqrt{1-2D^{1/4}}, \qquad z_2 = \sqrt{1+2D^{1/4}}. \tag{A5}$$

From z_1 we obtain the condition

$$D \leqslant 1/16, \tag{A6}$$

i.e., the WKB approximation is valid for weak noise strength. The exact value of integral

$$\Phi \equiv \int_0^{z_1} dx\sqrt{U(x)-\varepsilon_0} \tag{A7}$$

in Eq. (A2) is given by

$$\Phi = \frac{1}{3}z_2\left[\mathcal{E}\left(\frac{z_1^2}{z_2^2}\right) - 2D^{1/4}\mathcal{K}\left(\frac{z_1^2}{z_2^2}\right)\right], \tag{A8}$$

where $\mathcal{K}$ denotes the complete elliptic integral of the first kind

$$\mathcal{K}(m) \equiv \int_0^{\pi/2} (1 - m\sin^2\theta)^{-1/2} d\theta, \tag{A9}$$

and $\mathcal{E}$ denotes the complete elliptic integral of the second kind

$$\mathcal{E}(m) \equiv \int_0^{\pi/2} (1 - m\sin^2\theta)^{1/2} d\theta. \tag{A10}$$

Hence, the final result reads

$$\Delta\lambda = \frac{2D^{1/2}}{\pi}\exp\left(-\frac{2\Phi}{D^{1/2}}\right). \tag{A11}$$

We mention that we checked the correctness of Eq. (A8) numerically, too. Moreover, for $D\to 0$ one finds $\Phi\to 1/3$.

APPENDIX B: FISHER-EIGEN PROCESS AND MODERATE TO STRONG NOISE

We intend to calculate the rate for the Fisher-Eigen process at moderate to strong noise. To this end, we use Schrödinger's time-independent perturbation theory. In the first step we split operator $\hat{h}\equiv\hat{H}_{\mathrm{FE}}/D$,

$$\hat{h} = \hat{h}^0 + \alpha\hat{h}^1, \tag{B1}$$

into an anharmonic oscillator part $\hat{h}^0$ and a perturbation (the barrier) $\hat{h}^1$, that is,

$$\hat{h}^0 = -\frac{d^2}{dx^2} + \frac{x^4}{4D}, \quad \hat{h}^1 = -\frac{x^2}{2D}. \tag{B2}$$

By setting $\alpha=1$ we obtain the original problem. In order to calculate an approximation $\mu_0^{(0)}$ for the ground-state eigenvalue μ_0 of the anharmonic oscillator (corresponding to the situation, when there is no barrier, $\alpha=0$), we apply the Ritz method using the Gaussian test function

$$\psi_c(x) = \left(\frac{2c}{\pi}\right)^{1/4}\exp(-cx^2), \tag{B3}$$

where c denotes the variation parameter. By applying the Ritz condition to

$$\langle h^0\rangle \equiv \int_{-\infty}^{\infty} dx\,\psi_c^*\hat{h}^0\psi_c = c + \frac{3}{64c^2D}, \tag{B4}$$

we get

$$c = \frac{1}{2}\left(\frac{3}{4D}\right)^{1/3} \quad\Rightarrow\quad \mu_0^{(0)} = \frac{3}{4}\left(\frac{3}{4D}\right)^{1/3}. \tag{B5}$$

Using the test function

$$\chi_c(x) = 2\left(\frac{2c^3}{\pi}\right)^{1/4} x\exp(-cx^2) \tag{B6}$$

orthogonal to ψ_c, we find

$$\mu_1^{(0)} = \frac{11}{4}\left(\frac{3}{4D}\right)^{1/3} \quad\Rightarrow\quad \Delta\mu^{(0)} \equiv \mu_1^{(0)} - \mu_0^{(0)} = \left(\frac{6}{D}\right)^{1/3}. \tag{B7}$$

The result for the difference of eigenvalues in Eq. (B7) can be used to calculate a first estimate for the Fisher-Eigen escape rate, $k^{\mathrm{FE}}\approx\Delta\mu^{(0)}D/2$. In the remaining part, we calculate the corrections corresponding to $O(1/D)$ by following the standard procedure of quantum mechanical time-independent perturbation theory. From

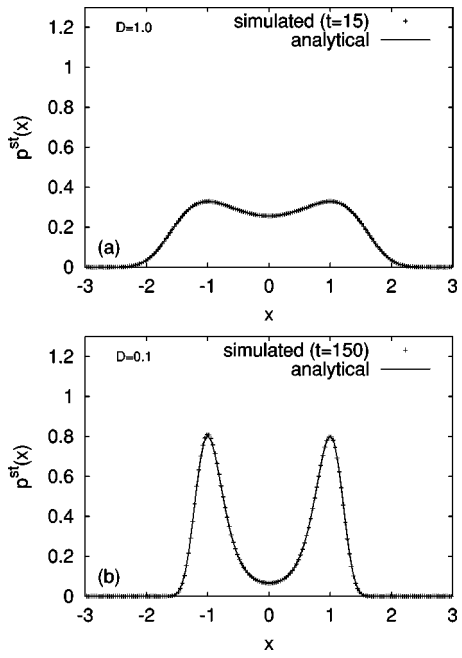

FIG. 6. Comparison of the exact time-independent solution $p^{st}(x)=\exp[-U(x)/D]/\mathcal{Z}^{st}$ of the Smoluchowski equation with numerically obtained stationary solutions for different values of the noise parameter D. The stationary normalization constants $\mathcal{Z}^{st}$ were numerically calculated as $\mathcal{Z}^{st}=3.905$ in (a) and $\mathcal{Z}^{st}=15.170$ in (b).

$$\mu_0^{(1)} = \int_{-\infty}^{\infty} dx\,\psi_c^*\hat{h}^1\psi_c = -\frac{1}{2}\left(\frac{1}{6D^2}\right)^{1/3}, \tag{B8a}$$

$$\mu_1^{(1)} = \int_{-\infty}^{\infty} dx\,\chi_c^*\hat{h}^1\chi_c = -\frac{1}{2}\left(\frac{9}{2D^2}\right)^{1/3}, \tag{B8b}$$

we get (for $\alpha=1$)

$$\Delta\mu \approx \Delta\mu^{(0)} + \alpha(\mu_1^{(1)} - \mu_0^{(1)}) = \left(\frac{6}{D}\right)^{1/3} - \left(\frac{1}{6D^2}\right)^{1/3}. \tag{B9}$$

We remark that this approximative result can, in principle, only be valid as long as $D>1/36$, because otherwise the rate $k^{\mathrm{FE}}=\Delta\mu D/2$ would become negative.

APPENDIX C: NUMERICAL METHODS

In our numerical simulations of the PDE we used a simple algorithm characterized as follows.

(1) *Discretization*. Spatial derivatives are realized by symmetric quotients, that is, $\partial p(x,t)/\partial x = [p(x+dx,t)-p(x-dx,t)]/(2dx)$ and $\partial^2 p(x,t)/\partial x^2 = [p(x+dx,t)-2p(x,t)+p(x-dx,t)]/dx^2$. Partial time derivatives are realized by forward quotients, $\partial p(x,t)/\partial t = [p(x,t+dt)-p(x,t)]/dt$. In all simulations we used a spatial interval $\Omega=[-5,5]$ with 301 equidistant spatial grid points (with distance dx). The time step dt was always chosen as $dt=0.05dx^2$. Furthermore, we fixed the boundary values $p(\pm 5,t)\equiv 0$.

(2) *Non-negativity*. If the probability density becomes negative at some grid point (x,t) during the simulation, we set $p(x,t)=0$.

(3) *Renormalization*. After each integration step the probability density at each grid point is multiplied by a constant such that $\int_\Omega dx p(x,t)=1$ holds.

There exist more refined numerical methods for these types of problems, for our purpose, however, the above algorithm proved to be completely satisfactory. For example, we plotted in Fig. 6 both the exactly known stationary solutions of the Smoluchowski equation and the numerically obtained solution. As can be deduced, there occurs an excellent agreement between the numerics and the approximation.

We also note, that we used harmonic test functions $U(x)=\omega^2 x^2/2$ in order to check the temporal behavior of the algorithm. This is possible, since for both the Smoluchowski and the Fisher-Eigen equation one can find explicit time-dependent solutions of the form

$$p(x,t)=\mathcal{Z}(t)^{-1}\exp[-\beta(t)U(x)] \tag{C1}$$

corresponding to the special case of Gaussian initial conditions (see Ref. [32] for further details).

[1] H.A. Kramers, Physica (Amsterdam) **7**, 284 (1940).
[2] P. Hänggi, P. Talkner, and M. Borkovec, Rev. Mod. Phys. **62**, 251 (1990).
[3] V.I. Melnikov, Phys. Rep. **209**, 1 (1991).
[4] A.N. Malakhov and A.L. Pankratov, *Advances in Chemical Physics* (Wiley Interscience, New York, 2002), Vol. 121, pp. 357–438.
[5] L. Gammaitoni, P. Hänggi, P. Jung, and F. Marchesoni, Rev. Mod. Phys. **70**, 223 (1998).
[6] D.B. Fogel, *Evolutionary Computation—Towards a New Philosophy of Machine Intelligence* (IEEE Press, Piscataway, NJ, 1995).
[7] J.R. Koza, *Genetic Programming: On the Programming of Computers by Means of Natural Selection* (MIT Press, Cambridge, MA, 1992).
[8] I. Rechenberg, *Evolutionsstrategien—Optimierung Technischer Systeme nach Prinzipien der Biologischen Information*, Stuttgart-Bad Cannstatt (Friedrich Frommann Verlag, Günter Holzboog, K.G., 1973).
[9] S. Kirkpatrick, C.D. Gelatt, Jr., and M.P. Vecchi, Science **220**, 671 (1983).
[10] G.H. Johannesson, T. Bligaard, A.V. Ruban, H.L. Skriver, K.W. Jacobson, and J.K. Nørskov, Phys. Rev. Lett. **88**, 255506 (2002).
[11] A. Einstein and M. von Smoluchowski, *Untersuchungen über die Theorie der Brownschen Bewegung/Abhandlungen über die Brownsche Bewegung und Verwandte Erscheinungen*, 3rd ed. (Harri Deutsch, Frankfurt, 1999), Vol. 199.
[12] S. Chandrasekhar, Rev. Mod. Phys. **15**, 1 (1943).
[13] R.A. Fisher, *The Genetical Theory of Natural Selection* (Oxford University Press, New York, 1930).
[14] M. Eigen, Naturwissenschaften **58**, 465 (1971).
[15] T. Boseniuk, W. Ebeling, and A. Engel, Phys. Lett. A **125**, 307 (1987).
[16] T. Asselmeyer, W. Ebeling, and H. Rosé, Phys. Rev. E **56**, 1171 (1997).
[17] T. Asselmeyer and W. Ebeling, Biosystems **41**, 167 (1996).
[18] R. Feistel and W. Ebeling, *Evolution of Complex Systems* (Kluwer Academic, Dordrecht, 1989).
[19] *Dynamik, Evolution, Strukturen-Nichtlineare Dynamik und Statistik komplexer Strukturen*, edited by J.A. Freund, Vol. 50 of Wissenschaftliche Schriftenreihe Physik (Verlag Dr. Köster, Berlin, 1996).
[20] F. Schweitzer, W. Ebeling, H. Rosé, and O. Weiss, Evol. Comput. **5**, 419 (1998).
[21] A. Reimann and W. Ebeling, Phys. Rev. E **65**, 046106 (2002).
[22] M. Bernstein and L.S. Brown, Phys. Rev. Lett. **52**, 1933 (1984).
[23] P. Hänggi and H. Thomas, Phys. Rep. **88**, 207 (1982).
[24] L.F. Favella, Ann. Inst. Henri Poincaré **VII**, 77 (1967).
[25] H. Tomita, A. Ito, and H. Kidachi, Prog. Theor. Phys. **56**, 786 (1976).
[26] H. Kalka and G. Soff, *Supersymmetrie* (Teubner, Leipzig, 1997).
[27] F. Marchesoni, P. Sodano, and M. Zannetti, Phys. Rev. Lett. **61**, 1143 (1988).
[28] L. Schimansky-Geier, H. Hempel, R. Bartussek, and C. Zülicke, Z. Phys. B: Condens. Matter **96**, 417 (1995).
[29] S.A. Gurvitz, Phys. Rev. A **38**, 1747 (1988).
[30] P. Hänggi, U. Weiss, and P.S. Riseborough, Phys. Rev. A **34**, 4558 (1986).
[31] U. Weiss and W. Haeffner, Phys. Rev. D **27**, 2916 (1983).
[32] J. Dunkel, W. Ebeling, and L. Schimansky-Geier (unpublished).